

Cite this: *Chem. Sci.*, 2023, 14, 9010

All publication charges for this article have been paid for by the Royal Society of Chemistry

Received 26th May 2023

Accepted 14th July 2023

DOI: 10.1039/d3sc02668j

rsc.li/chemical-science

Boroles from alumes: accessing boroles with alkyl-substituted backbones *via* transtrielation†

Josina L. Bohlen,^{ab} Lukas Endres,^{ab} Regina Drescher,^{ab} Krzysztof Radacki,^{ab} Maximilian Dietz,^{ab} Ivo Krummenacher^{ab} and Holger Braunschweig^{ab}*

The alumole $\text{Cp}^{\text{3t}}\text{AlC}_4\text{Et}_4$ ($\text{Cp}^{\text{3t}} = 1,2,4\text{-tris(tert-butyl)cyclopentadienyl}$) is reported to be capable of transferring its butadiene moiety to aryl(dihalo)boranes to generate boroles through aluminum–boron exchange. The products feature a rare alkyl-substituted backbone, which, as shown in other examples, often leads to dimerization due to insufficient steric protection of the antiaromatic borole ring. Sterically crowded aryl groups bound to the boron atom are shown to prevent dimerization, allowing access to the first monomeric derivatives of this type. Results from UV-vis spectroscopy, electrochemistry, and DFT calculations reveal that the alkyl substituents cause remarkable modifications in the optical and electronic properties of the boroles compared to their perarylated counterparts.

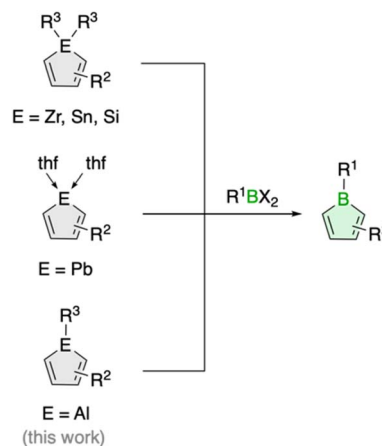
Introduction

The transfer of organic ligands from one metal to another, known as transmetalation, is an important organometallic reaction with great utility in synthetic chemistry.¹ Not only is it a crucial step in Nobel Prize-winning palladium-catalyzed cross-coupling reactions,² it also enables the preparation of a variety of organometallic compounds of both main group and transition metals.¹ For instance, this strategy has greatly increased the synthetic accessibility of unsaturated five-membered organometallic heterocycles, so called metalloles,³ which are increasingly finding applications as light-emitting materials due to their unique optoelectronic properties.⁴ In the most common reaction process, the metalloles are generated by reacting zirconacyclopentadienes with metal or p-block element halides.⁵ The reaction, named after its developers Fagan and Nugent, is characterized by high efficiency and great generality, especially in the preparation of five-membered heterocycles of the heavier p-block elements.⁵ Lighter analogues such as boroles are also accessible, but the reaction often fails, and so far only very few examples have been described.⁶

Boroles, which have a distinct antiaromatic character, are generally more readily available from other metalloles, such as stannoles.⁷ Besides the cyclization of 1,4-dilithio-1,3-dienes with (organo)boron halides, transmetalation *via* tin–boron

exchange is probably the most common method for the synthesis of monocyclic boroles, especially for derivatives with aryl groups in the carbon backbone.⁷ Further metallacycle transfers to boron have been reported for silicon analogues (Scheme 1).⁸ These routes are particularly valuable for the preparation of dibenzannulated boroles, also known as 9-borafluorenes.⁹ Moreover, a unique transmetalation of a plumbole with boron trifluoride etherate was described,¹⁰ yielding a borole derivative with a B–F bond that was not accessible by other methods.¹¹ It further featured silyl groups at the 2,5 positions, substituents known to electronically interfere with the ability of stannoles to transfer their diene moiety.¹²

Such alternative transmetalation reactions may thus prove advantageous for the introduction of new functionalities



Scheme 1 Generic scheme for borole synthesis *via* metallacycle transfer.

^aInstitute for Inorganic Chemistry, Julius-Maximilians-Universität Würzburg, Am Hubland, 97074 Würzburg, Germany. E-mail: h.braunschweig@uni-wuerzburg.de

^bInstitute for Sustainable Chemistry & Catalysis with Boron, Julius-Maximilians-Universität Würzburg, Am Hubland, 97074 Würzburg, Germany

† Electronic supplementary information (ESI) available: Synthetic procedures, NMR and UV-vis spectra, electrochemical, X-ray crystallographic and computational details. CCDC 2263083–2263085. For ESI and crystallographic data in CIF or other electronic format see DOI: <https://doi.org/10.1039/d3sc02668j>

around the borole ring that can lead to new properties. Herein, we show that alumoles, the heavier group 13 homologues of boroles,¹³ can serve as effective precursors for the preparation of boroles with alkyl substituents in the backbone. Alkyl-substituted borole derivatives are rare and have only been observed in equilibrium with their dimeric Diels–Alder cyclo-adducts.⁶ By incorporating ethyl substituents at the borole backbone and a bulky organic substituent at boron, we were able to obtain the first examples of monomeric 2,3,4,5-tetraalkylboroles. Moreover, we investigated the influence of the alkyl substituents on the chemical and physical properties of the boroles with a combination of spectroscopic, electrochemical and computational methods.

Results and discussion

Borole synthesis from alumoles

We have recently introduced a new alumole derivative (**1**) with a bulky 1,2,4-tris(*tert*-butyl)cyclopentadienyl (Cp^{3t}) ligand at the aluminum atom, which exists as a monomer both in solution and in the solid state.¹⁴ Its properties are largely tied to the fluxional behavior of the Cp ligand, which ensures accessibility to the electrophilic Al center.¹⁵ We reasoned that the lower electronegativity of aluminum compared to boron and the lability of the aluminum–carbon bonds might lead to facile transfer of the diene unit to the boron atom.¹⁶

Treatment of **1** with the sterically hindered aryl(dibromo)boranes MesBBr_2 ($\text{Mes} = 2,4,6\text{-trimethylphenyl}$)¹⁷ and DurBBr_2 ($\text{Dur} = 2,3,5,6\text{-tetramethylphenyl}$)¹⁸ led to no immediate reaction in benzene solutions, but a slow conversion to a new product was observed at higher temperatures. The new broad ^{11}B NMR resonances at $\delta(^{11}\text{B}) = 76.5$ (2) and 77.6 ppm (3), respectively, are consistent with formation of the expected

borole rings (Fig. 1).⁷ Despite full conversion of alumole **1**, isolation of the boroles proved challenging because of the difficulty in separating the hydrocarbon-soluble aluminum species $\text{Cp}^{3t}\text{AlBr}_2$, which is formed as a side product. After numerous attempts to induce precipitation of the aluminum compound by adduction formation, we found that the addition of the cyclic(alkyl)(amino)carbene CAAC^{Me} (1-(2,6-diisopropylphenyl)-3,3,5,5-tetramethylpyrrolidin-2-ylidene)¹⁹ results in an insoluble adduct that can be easily removed by filtration. By this process, the corresponding air-sensitive boroles were obtained in analytically pure form in yields exceeding 90% (Fig. 1).[‡] Despite the oily nature of the products, we were able to obtain crystals suitable for X-ray diffraction analysis in the case of **3** (Fig. 1). Although problems with refinement (*i.e.* disorder across the crystallographic mirror plane) preclude a detailed analysis of the complete structure, the solution is sufficient to discuss the bond parameters of the central borole ring (see ESI[†] for details). The alternating single and double carbon–carbon bond lengths of 1.342(7), 1.522(7), and 1.349(6) Å show no or only small differences to those of the perarylated borole $\text{MesBC}_4\text{Ph}_4$; although the C–C single bond is statistically shorter (1.522(7) *vs.* 1.560(2) Å).²⁰ The boron–carbon bonds as well as the 73.6° twist of the duryl group relative to the borole ring are likewise comparable. The effect of the ethyl substituents on the conjugation in the ring is thus not readily apparent, which may also be due – at least in part – to the greater uncertainty in the bond lengths of **3**. Boroles **2** and **3** appear red, corresponding to light absorption in the green region of the spectrum ($\lambda_{\text{max}} = 505$ nm and $\lambda_{\text{max}} = 500$ nm, respectively). The UV-vis absorptions are thus significantly blue-shifted compared to the perarylated boroles PhBC_4Ph_4 ($\lambda_{\text{max}} = 560$ nm)²¹ and $\text{MesBC}_4\text{Ph}_4$ ($\lambda_{\text{max}} = 578$ nm),²⁰ which are blue and green solids, respectively. These lowest energy absorptions are associated with HOMO–LUMO transitions, demonstrating that the alkyl-substituted backbone in **2** and **3** is what causes the larger optical band gap.²² Cyclic voltammetry, which provides a way to estimate the LUMO energy through the measurement of the reduction potential of a molecule, allowed a better understanding of the relative energies of the frontier orbitals. Boroles **2** and **3** were found to undergo irreversible reduction events at -2.33 and -2.57 V *vs.*



Fig. 1 Borole synthesis from alumoles and molecular structure of **3** (ellipsoids at 50% probability). Selected bond lengths (Å) and angles (°): B1_1–C1_2 1.603(6), B1_1–C2_1 1.558(7), B1_1–C5_1 1.579(8), C2_1–C3_1 1.349(6), C3_1–C4_1 1.522(7), C4_1–C5_1 1.342(7); C5_1–B1_1–C2_1 104.5(4).



Fig. 2 Cyclic voltammograms of **2**, **3**, and **4** in dichloromethane solution showing the first reduction events (supporting electrolyte: $[\text{NBu}_4][\text{PF}_6]$ (0.1 M), scan rate: 250 mV s^{-1}).

Fc/Fc^+ , respectively, which are cathodically shifted by more than 0.6 V relative to those of PhBC_4Ph_4 ($E_{1/2} = -1.61$ V vs. Fc/Fc^+)²³ and $\text{MesBC}_4\text{Ph}_4$ ($E_{1/2} = -1.69$ V vs. Fc/Fc^+ , Fig. 2).²⁰ The more negative reduction potentials of the alkyl-substituted boroles indicate that their LUMOs are significantly higher in energy than those of the aryl-substituted boroles, contributing to the larger HOMO–LUMO gaps (see DFT results below). To the best of our knowledge, boroles **2** and **3** represent the first monocyclic borole derivatives with alkyl substituents on the diene backbone. Previous derivatives were shown to undergo spontaneous Diels–Alder dimerization due to insufficient steric shielding by the ring substituents (*c.f.* PhBC_4Me_4 or PhBC_4Et_4).⁶

A range of other dihaloboranes was evaluated as reagents to assess the scope of the transmetalation reaction. We found that boroles **2** and **3** could also be obtained by using dichloroboranes instead of the dibromoboranes MesBBr_2 and DurBBr_2 , respectively. In a similar manner, (dibromoboryl)ferrocene (FcBBr_2)²⁴ reacts cleanly with alumole **1** to afford the borole product **4** (73% yield; Fig. 1). In this case, the transformation proceeds rapidly at room temperature without the need for heating. Because of its propensity to form oils, borole **4** was not readily susceptible to crystallization and was instead isolated as a dark red oil. The ^{11}B NMR resonance at $\delta(^{11}\text{B}) = 54.7$ is consistent with the presence of an intramolecular iron–boron interaction in borole **4**, as observed in many other borylferrocenes including FcBC_4Ph_4 ($\delta(^{11}\text{B}) = 47.4$ ppm).^{21,25} As expected from this stabilizing donor–acceptor interaction, the boron atom in **4** becomes less electrophilic and is therefore reduced at more negative potential ($E_{\text{pc}} = -2.97$ V) than its *B*-aryl substituted analogues **2** and **3** (Fig. 2). Borole **4** has been further characterized by high-resolution mass spectrometry (HRMS), multinuclear NMR and UV-vis spectroscopy. The UV-vis spectrum of **4** in dichloromethane solution shows two absorption bands at $\lambda_{\text{max}} = 472$ and 372 nm, which are again blue-shifted compared to those of the phenyl-substituted counterpart (FcBC_4Ph_4 ; $\lambda_{\text{max}} = 490$ and 390 nm).^{7d,21} Similar to boroles **2** and **3**, borole **4** does not form an adduct with thf.

In addition, we have tested the aluminum–boron exchange reaction to access the phenyl-substituted derivative PhBC_4Et_4 (**5**), previously reported by Martin and coworkers.^{6c} The compound was isolated as its Diels–Alder dimer, but in solution was shown to be in equilibrium with its monomeric variant. Using our protocol, addition of dibromo(phenyl)borane to **1** resulted in complete conversion of the alumole within a few minutes at room temperature (Fig. 3). After work up using CAAC^{Me} to remove the aluminum by-product, we obtained borole **5** as carbene adduct **5a** in 44% yield. The base-free borole **5** could not be isolated cleanly. The orange adduct was amenable to crystallization. Its molecular structure, as determined by single-crystal X-ray diffraction, shows no unusual features compared to other carbene–borole adducts, with unobtrusive B–C(carbene) (1.654(2) Å), endocyclic B–C (av. 1.651(3) Å), single (1.485(2) Å) and double C–C (av. 1.353(3) Å) bond lengths.²⁶ In addition, the ^{11}B NMR signal at $\delta = -3.9$ ppm is in a typical range seen for other borole adducts.²⁶ The isolation of borole adduct **5a** reaffirms that the Diels–Alder dimer of **5** exists in solution in equilibrium with its monomer.^{6c}



Fig. 3 Synthesis of borole adducts **5a** and **6a** through trapping reactions of the borole monomers **5** and **6**, respectively (top). Molecular structures of **5a** and **6a** with displacement ellipsoids shown at 50% probability (bottom; H atoms omitted for clarity).

Finally, one last variation in the steric demand of the aryl group in the dihaloborane reagent was explored. Dichloro(*ortho*-tolyl)borane²⁷ was reacted with alumole **1** in benzene, resulting in immediate formation of a purple solution. Unfortunately, standard workup with one equivalent of the carbene CAAC^{Me} yielded only an impure product, contaminated with the aluminum species Cp^3AlCl_2 and the carbene adduct of the expected borole **6**. Numerous attempts to isolate **6** in pure form proved unsuccessful. In the process, we found that utilizing bromide instead of chloride in the borane reagent did not bring about a successful aluminum–boron exchange reaction. We thus added two equivalents of the carbene to selectively obtain borole adduct **6a** (Fig. 3). Despite the *ortho*-methyl substituent on the aryl group, adduct formation proceeds smoothly and **6a** can be obtained in 33% yield as an orange-red solid. The transformation is reflected in a characteristic low-frequency ^{11}B NMR signal at $\delta(^{11}\text{B}) = -2.7$ ppm, consistent with a tetrahedral boron atom.^{7,26} The Lewis acid–base structure was revealed by X-ray diffraction analysis and consists of a boron–carbene bond of 1.680(2) Å.²⁶ The borole intraring distances are comparable to those of **5a**.

Tin–boron exchange

To determine if the aluminum–boron exchange has an advantage over the tin–boron exchange, we also attempted to synthesize the new alkyl boroles *via* this more conventional approach. The comparison revealed some interesting differences between the two methods.



While the synthesis of boroles **2**, **4**, and **6** from the stannole $\text{Me}_2\text{SnC}_4\text{Et}_4$ succeeded,²⁸ it was unsuccessful for the duryl-(3) and phenyl-substituted derivatives (**5**), using both dichloro- and dibromoboranes. The successful transformations occurred with excellent yields of over 90% (detailed synthetic procedures can be found in the ESI†). In direct comparison, alumole **1** appears to be equally effective as the stannole in transferring the 1,2,3,4-tetraethyl-1,3-butadiene-1,4-diyl fragment for the formation of boroles. However, the use of the Al-B exchange method is accompanied by the formation of highly soluble aluminum dihalides as by-products, which is a drawback to consider, especially in light of the additional use of CAAC^{Me} and the synthesis of alumole **1**. The presence of these aluminum species hindered the isolation of the *o*-tolyl derivative **6**. However, in this case, the tin-boron exchange reaction proved effective, allowing us to isolate and characterize the free borole **6**. We found that it exists in solution in both monomeric and dimeric forms that interconvert on the NMR timescale. At 70 °C, the equilibrium shifts almost completely to the side of the monomer ($\delta(^{11}\text{B}) = 74.6$ ppm). At lower temperatures, a characteristic ^{11}B NMR signal for the dimer is detectable at -11.3 ppm, while the signal for the non-bridgehead boron atom is masked by the monomer signal.⁶ The shift of the equilibrium towards the monomeric form at higher temperatures is also visually evident as the color of the solution gradually intensifies to a deeper shade of purple. Furthermore, the monomeric borole form is readily detectable in the mass spectrum ($m/z = 266.2195$). No single crystals suitable for X-ray diffraction analysis could be obtained from either the monomeric or dimeric forms.

DFT calculations

To better understand the effects of the alkyl substituents on the nature and relative energies of the frontier orbitals, DFT calculations were undertaken. 1-Mesityl-2,3,4,5-tetraphenylborole ($\text{MesBC}_4\text{Ph}_4$, abbreviated as **2Ph₄** in the following),²⁰ which has the same boron substituent as borole **2** but instead a tetraphenyl-substituted backbone, was as an ideal candidate for comparison. The PBE0-D3(BJ) functional²⁹ was chosen because it provides geometric parameters that agree well with those obtained from X-ray diffraction analysis of **2Ph₄**. While experimental data are lacking for **2**, the geometrically optimized structure of **2** shows no significant differences in bond lengths or angles in the planar BC_4 ring compared to **2Ph₄** (see Table S1 in the ESI†). The alternating carbon-carbon single (1.531 Å) and double bonds (1.353 Å) are also in line with the structural study of the duryl derivative **3**. The most striking differences between the two boroles were found in the energy of their frontier orbitals, which are displayed in Fig. 4. The ethyl groups on the borole ring in **2** considerably increase the LUMO energy compared to **2Ph₄** and thus also increase the HOMO–LUMO gap. The presence of tetraphenyl substitution in the backbone of compound **2Ph₄** leads to a more delocalized LUMO, extending into the π systems of the phenyl rings. This extension leads to a greater stabilization of its LUMO compared to that of **2**.¹² The difference in the relative orbital energies of the two boroles can also be attributed to the different inductive



Fig. 4 Frontier molecular orbitals and relative energies (in eV) for **2** and **2Ph₄**, calculated at the PBE0-D3(BJ)/6-311+G(d,p) level of theory.

effects of the backbone substituents. The phenyl groups, for which resonance conjugation with the borole ring is impaired due to their propeller-like arrangement, exert a negative inductive effect, while the ethyl groups exert a positive inductive effect. As a result, the energies of the frontier orbitals of **2** are further destabilized compared to **2Ph₄**. The differences in the relative energies of the orbitals are consistent with the electrochemical and UV-vis absorption data of **2**, indicating a higher LUMO level and larger band gap, respectively, compared to **2Ph₄**.

Furthermore, natural bond orbital (NBO) analysis³⁰ shows that the inductive electron donation from the ethyl substituents only marginally reduces the positive charge of the boron atom in **2** (+1.017) compared to that of **2Ph₄** (+1.034). Similarly, the negative charge on the carbon atoms in the BC_4 ring is only slightly higher in **2** (see ESI† for details). As evident from nucleus-independent chemical shift (NICS) calculations,³¹ the more electron-rich alkyl backbone in **2** results in a somewhat more antiaromatic borole than **2Ph₄**; borole **2** has a NICS(0) value of 16.38 ppm, while that for **2Ph₄** is 14.75 ppm.^{9b,32} The NICS values calculated at larger distances from the ring center, primarily measuring the contribution from the π -system, come to the same conclusion (see ESI† for NICS_{zz} scan profiles).

Taken together, the ethyl substituents significantly perturb the electronic structure of the borole relative to perarylated derivatives. These ethyl-substituted boroles become significantly more electron rich, resulting in a higher LUMO energy level and a larger HOMO–LUMO gap.

Conclusions

In summary, we have developed a protocol for borole synthesis *via* aluminum–boron exchange. Starting from a 2,3,4,5-tetraethyl-substituted alumole, the procedure enabled the synthesis of several borole derivatives with alkyl substituents in the backbone, including the first monomeric examples.



Computational and experimental data indicate that they are inferior acceptors and have a larger HOMO–LUMO gap than their perarylated borole derivatives. Our work thus illustrates how the diene substituents can be used to modify the optical and electronic characteristics of boroles.

Data availability

The data that supports the findings of this study are available on reasonable request from the corresponding author.

Author contributions

J. L. B. synthesized and characterized the compounds and carried out spectroscopic studies. L. M. completed the DFT calculations. R. D. performed preliminary studies. K. R. and M. D. performed X-ray crystallographic analyses. I. K. performed electrochemical experiments and wrote the original draft of the manuscript, which was edited by all authors. H. B. conceived and supervised the research.

Conflicts of interest

There are no conflicts of interest to declare.

Acknowledgements

Financial support from the Deutsche Forschungsgemeinschaft (DFG) is gratefully acknowledged (project numbers BR1149/25-1 and 466754611). J. L. B. and L. M. thank the Fonds der Chemischen Industrie (FCI) for a Kekulé fellowships. M. D. thanks the Studienstiftung des deutschen Volkes for a doctoral fellowship.

Notes and references

‡ We found that certain borole samples contained small paramagnetic impurities that likely originate from soluble CAAC-stabilized aluminum radicals.

- (a) D. V. Partyka, *Chem. Rev.*, 2011, **111**, 1529–1595; (b) S. C. Rasmussen, *ChemTexts*, 2021, **7**, 1–8.
- See, for instance: C. C. C. Johansson Seechurn, M. O. Kitching, T. J. Colacot and V. Snieckus, *Angew. Chem., Int. Ed.*, 2012, **51**, 5062–5085.
- For selected reviews, see: (a) J. Dubac, A. Laporterie and G. Manuel, *Chem. Rev.*, 1990, **90**, 215–263; (b) W. Ma, C. Yu, T. Chen, L. Xu, W.-X. Zhang and Z. Xi, *Chem. Soc. Rev.*, 2017, **46**, 1160–1192.
- See, for instance: (a) Y. Cai, A. Qin and B. Z. Tang, *J. Mater. Chem. C*, 2017, **5**, 7375–7389; (b) E. Rivard, *Chem. Rec.*, 2020, **20**, 640–648; (c) S. Santra, *ChemistrySelect*, 2020, **5**, 9034–9058.
- (a) P. J. Fagan, W. A. Nugent and J. C. Calabrese, *J. Am. Chem. Soc.*, 1994, **116**, 1880–1889; (b) X. Yan and C. Xi, *Acc. Chem. Res.*, 2015, **48**, 935–946; (c) X. Yan and C. Xi, *Coord. Chem. Rev.*, 2017, **350**, 275–284.
- (a) P. J. Fagan, E. G. Burns and J. C. Calabrese, *J. Am. Chem. Soc.*, 1988, **110**, 2979–2981; (b) J. J. Baker, K. H. M. Al Furajji, O. Tara Liyanage, D. J. D. Wilson, J. L. Dutton and C. D. Martin, *Chem. – Eur. J.*, 2019, **25**, 1581–1587; (c) X. Su, J. J. Baker and C. D. Martin, *Chem. Sci.*, 2020, **11**, 126–131.
- For borole reviews, see: (a) J. Eisch, *Adv. Organomet. Chem.*, 1996, **39**, 355–391; (b) A. Steffen, R. M. Ward, W. D. Jones and T. B. Marder, *Coord. Chem. Rev.*, 2010, **254**, 1950–1976; (c) H. Braunschweig and T. Kupfer, *Chem. Commun.*, 2011, **47**, 10903–10914; (d) H. Braunschweig, I. Krummenacher and J. Wahler, *Adv. Organomet. Chem.*, 2013, **61**, 1–53; (e) A. Wakamiya and S. Yamaguchi, *Bull. Chem. Soc. Jpn.*, 2015, **88**, 1357–1377; (f) J. H. Barnard, S. Yruegas, K. Huang and C. D. Martin, *Chem. Commun.*, 2016, **52**, 9985–9991; (g) B. Su and R. Kinjo, *Synthesis*, 2017, **49**, 2985–3034; (h) W. Zhang, B. Zhang, D. Yu and G. He, *Sci. Bull.*, 2017, **62**, 899–900; (i) A. Wakamiya in *Main Group Strategies towards Functional Hybrid Materials* ed. T. Baumgartner and F. Jäkle, John Wiley & Sons Ltd., Hoboken (New Jersey), 2018, vol. 1, pp. 1–26; (j) C. Hong, J. Baltazar and J. D. Toivola, *J. Org. Chem.*, 2022, e202101343.
- (a) U. Gross and D. Kaufmann, *Chem. Ber.*, 1987, **120**, 991–994; (b) A. Wakamiya, K. Mishima, K. Ekawa and S. Yamaguchi, *Chem. Commun.*, 2008, 579–581; (c) A. Hübner, M. Diefenbach, M. Bolte, H.-W. Lerner, M. C. Holthausen and M. Wagner, *Angew. Chem., Int. Ed.*, 2012, **51**, 12514–12518.
- (a) X. Su, T. A. Bartholome, J. R. Tidwell, A. Pujol, S. Yruegas, J. J. Martinez and C. D. Martin, *Chem. Rev.*, 2021, **121**, 4147–4192; (b) J. He, F. Rauch, M. Finze and T. B. Marder, *Chem. Sci.*, 2021, **12**, 128–147.
- M. Saito, T. Akiba, M. Kaneko, T. Kawamura, M. Abe, M. Hada and M. Minoura, *Chem. – Eur. J.*, 2013, **19**, 16946–16953.
- H. Braunschweig, C. Hörl, F. Hupp, K. Radacki and J. Wahler, *Organometallics*, 2012, **31**, 8463–8466.
- T. Heitkemper, L. Naß and C. P. Sindlinger, *Dalton Trans.*, 2020, **49**, 2706–2714.
- For the first report, see: J. J. Eisch and W. C. Kaska, *J. Am. Chem. Soc.*, 1962, **84**, 1501–1502. See, also: P. von Ragué Schleyer, P. K. Freeman, H. Jiao and B. Goldfuss, *Angew. Chem., Int. Ed. Engl.*, 1995, **34**, 337–340; T. Agou, T. Wasano, P. Jin, S. Nagase and N. Tokitoh, *Angew. Chem., Int. Ed.*, 2013, **52**, 10031–10034.
- R. Drescher, S. Lin, A. Hofmann, C. Lenczyk, S. Kachel, I. Krummenacher, Z. Lin and H. Braunschweig, *Chem. Sci.*, 2020, **11**, 5559–5564.
- R. Drescher, B. Ritschel, R. D. Dewhurst, A. Deifßenberger, A. Hofmann and H. Braunschweig, *Chem. Commun.*, 2021, 57, 7505–7508.
- Ligand exchanges between aluminum and boron atoms are well known. See, for instance: (a) J. Klosin, G. R. Roof, E. Y.-X. Chen and K. A. Abboud, *Organometallics*, 2000, **19**, 4684–4686; (b) J. Chen and E. Y.-X. Chen, *Dalton Trans.*, 2016, **45**, 6105–6110; (c) D. M. C. Ould, J. L. Carden, R. Page and R. L. Melen, *Inorg. Chem.*, 2020, **59**, 14891–14898.
- W. Haubold, J. Herdtle, W. Gollinger and W. Einholz, *J. Organomet. Chem.*, 1986, **315**, 1–8.



- 18 H. Braunschweig, Q. Ye and K. Radacki, *Chem. Commun.*, 2012, **48**, 2701–2703.
- 19 V. Lavallo, Y. Canac, C. Präsang, B. Donnadieu and G. Bertrand, *Angew. Chem., Int. Ed.*, 2005, **44**, 5705–5709.
- 20 H. Braunschweig, V. Dyakonov, J. O. C. Jimenez-Halla, K. Kraft, I. Krummenacher, K. Radacki, A. Sperlich and J. Wahler, *Angew. Chem., Int. Ed.*, 2012, **51**, 2977–2980.
- 21 H. Braunschweig, I. Fernández, G. Frenking and T. Kupfer, *Angew. Chem., Int. Ed.*, 2008, **47**, 1951–1954.
- 22 See, for instance: Z. Zhang, R. M. Edkins, M. Haehnel, M. Wehner, A. Eichhorn, L. Mailänder, M. Meier, J. Brand, F. Brede, K. Müller-Buschbaum, H. Braunschweig and T. B. Marder, *Chem. Sci.*, 2015, **6**, 5922–5927.
- 23 H. Braunschweig and I. Krummenacher in *Organic Redox Systems: Synthesis, Properties, and Applications*, ed. T. Nishinaga, John Wiley & Sons, Hoboken (New Jersey), 2016, pp. 503–519.
- 24 T. Renk, W. Ruf and W. Siebert, *J. Organomet. Chem.*, 1976, **120**, 1–25.
- 25 M. Scheibitz, M. Bolte, J. W. Bats, H.-W. Lerner, I. Nowik, R. H. Herber, A. Krapp, M. Lein, M. C. Holthausen and M. Wagner, *Chem. – Eur. J.*, 2005, **11**, 584–603.
- 26 H. Braunschweig, C.-W. Chiu, D. Gamon, K. Gruf, C. Hörl, T. Kupfer, K. Radacki and J. Wahler, *Eur. J. Inorg. Chem.*, 2013, 1525–1530.
- 27 W. Schacht and D. Kaufmann, *Chem. Ber.*, 1987, **120**, 1331–1338.
- 28 Y. Ura, Y. Li, Z. Xi and T. Takahashi, *Tetrahedron Lett.*, 1998, **39**, 2787–2790.
- 29 C. Adamo and V. Barone, *J. Chem. Phys.*, 1999, **110**, 6158–6170.
- 30 (a) J. P. Foster and F. Weinhold, *J. Am. Chem. Soc.*, 1980, **102**, 7211–7218; (b) A. E. Reed and F. Weinhold, *J. Chem. Phys.*, 1983, **78**, 4066–4073.
- 31 P. von Ragué Schleyer, C. Maerker, A. Dransfeld, H. Jiao and N. J. R. van Eikema Hommes, *J. Am. Chem. Soc.*, 1996, **118**, 6317–6318.
- 32 (a) A. Iida and S. Yamaguchi, *J. Am. Chem. Soc.*, 2011, **133**, 6952–6955; (b) J. O. C. Jimenez-Halla, E. Matito, M. Solà, H. Braunschweig, C. Hörl, I. Krummenacher and J. Wahler, *Dalton Trans.*, 2015, **44**, 6740–6747.

